

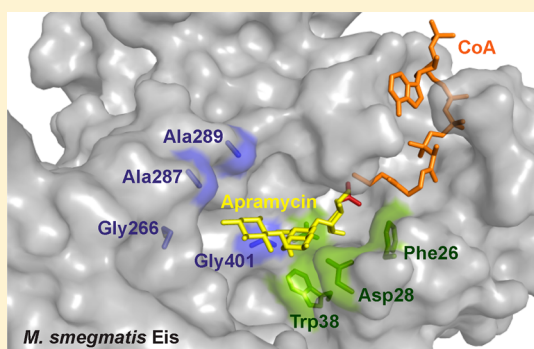
Aminoglycoside Multiacetylating Activity of the Enhanced Intracellular Survival Protein from *Mycobacterium smegmatis* and Its Inhibition

Wenjing Chen,^{†,‡} Keith D. Green,[†] Oleg V. Tsodikov,[§] and Sylvie Garneau-Tsodikova^{*,†,‡,§}

[†]Life Sciences Institute, 210 Washtenaw Avenue, [‡]Chemical Biology Doctoral Program, and [§]Department of Medicinal Chemistry, University of Michigan, Ann Arbor, Michigan 48109-2216, United States

S Supporting Information

ABSTRACT: The enhanced intracellular survival (Eis) protein improves the survival of *Mycobacterium smegmatis* (Msm) in macrophages and functions as the acetyltransferase responsible for kanamycin A resistance, a hallmark of extensively drug-resistant (XDR) tuberculosis, in a large number of *Mycobacterium tuberculosis* (Mtb) clinical isolates. We recently demonstrated that Eis from Mtb (Eis_Mtb) efficiently multiacetylates a variety of aminoglycoside (AG) antibiotics. Here, to gain insight into the origin of substrate selectivity of AG multiacetylation by Eis, we analyzed AG acetylation by Eis_Msm, investigated its inhibition, and compared these functions to those of Eis_Mtb. Even though for several AGs the multiacetylation properties of Eis_Msm and Eis_Mtb are similar, there are three major differences. (i) Eis_Msm diacetylates apramycin, a conformationally constrained AG, which Eis_Mtb cannot modify. (ii) Eis_Msm triacetylates paromomycin, which can be only diacetylated by Eis_Mtb. (iii) Eis_Msm only monoacetylates hygromycin, a structurally unique AG that is diacetylated by Eis_Mtb. Several nonconserved amino acid residues lining the AG-binding pocket of Eis are likely responsible for these differences between the two Eis homologues. Specifically, we propose that because the AG-binding pocket of Eis_Msm is more open than that of Eis_Mtb, it accommodates apramycin for acetylation in Eis_Msm, but not in Eis_Mtb. We also demonstrate that inhibitors of Eis_Mtb that we recently discovered can inhibit Eis_Msm activity. These observations help define the structural origins of substrate preference among Eis homologues and suggest that Eis_Mtb inhibitors may be applied against all pathogenic mycobacteria to overcome AG resistance caused by Eis upregulation.



According to the World Health Organization, more than 2 billion people, approximately one-third of the world's population, are infected with *Mycobacterium tuberculosis* (Mtb) bacilli that cause the highly contagious and life-threatening tuberculosis (TB). With almost 2 million deaths and 9 million new cases each year, the TB epidemic is one of the most devastating health problems worldwide. The rapidly emerging resistance to all of the available anti-TB drugs presents one of the biggest obstacles in treating the disease. Multidrug-resistant (MDR),^{1,2} extensively drug-resistant (XDR),^{3,4} extremely drug-resistant (XXDR),⁵ and more recently totally drug-resistant (TDR)⁵ strains of Mtb have been identified.

To develop novel strategies for fighting this notorious human pathogen, a better understanding of the basic biology of Mtb and its virulence is needed. While many laboratories successfully study Mtb, faster-dividing and nonpathogenic *Mycobacterium smegmatis* (Msm) has been used as a model mycobacterium to gain insight into Mtb mechanisms.^{6–8} The entire genomes of both Mtb^{9,10} and Msm have been sequenced and annotated. Msm shares not only more than 2000 homologues with Mtb and most of the Mtb virulence genes but also the same unusual cell wall structure.⁷ Hyper-

transformable Msm strain MC2 155 is now used as a convenient tool for mycobacterial genetics.

It was previously shown that upregulation of the Mtb enhanced intracellular survival (Eis) protein is responsible for resistance to the aminoglycoside (AG) kanamycin A (KAN), a hallmark of XDR-TB, in a significant fraction of KAN-resistant Mtb clinical isolates.¹¹ Eis homologues have been found in many pathogens and numerous mycobacterial species (Figure 1 and Figure S1 of the Supporting Information). When transformed into Msm, the *eis_Mtb* gene was found to increase intracellular survival of Msm in the human macrophage-like cell line U-937.¹² On the basis of both biochemical and structural analyses, we recently demonstrated that Eis_Mtb belongs to a novel family of hexameric acetyltransferases, whose tripartite fold is composed of two GCN5 N-acetyltransferase regions, only one of which is active, and a sterol carrier protein fold.¹³ All three regions contribute to the structure of the active site and the intricate substrate-binding cavity. We showed that

Received: April 7, 2012

Revised: May 29, 2012

Published: May 30, 2012



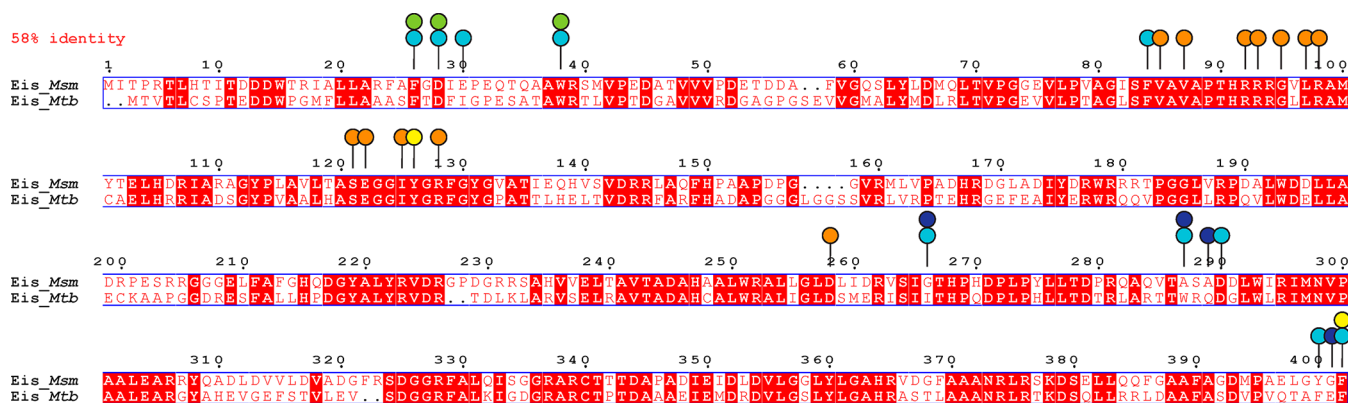


Figure 1. Sequence alignment of Eis_Msm from *Msm* strain MC2 155 and Eis_Mtb from *Mtb* strain H37Rv. The sequences of the two Eis homologues are 58% identical. On the basis of structural and mutagenesis studies of Eis_Mtb, the residues proposed to be involved in catalysis, in binding CoA, and in formation of the AG-binding pocket are marked with yellow, orange, and turquoise circles, respectively.¹³ Nonconserved residues in the AG-binding pockets of these two proteins are additionally marked with dark blue circles. Conserved residues in the AG-binding pockets of Eis_Msm and Eis_Mtb are marked with green circles.

Eis_Mtb has an unprecedented ability to acetylate multiple amines of many AGs. This multiacetylation is regiospecific; however, the substrate recognition and specificity rules for the N-acetylation remain unclear. Herein, in the hope that functional differences between Eis_Mtb and its closely genetically related, but not identical, homologue from *Msm* (Eis_Msm) will provide insight into the substrate recognition and N-acetylation specificity rules of the Eis family, we performed biochemical characterization of Eis_Msm. In addition, to probe the active site of Eis_Msm, we used AG-competitive acetylation inhibitors of Eis_Mtb that we recently discovered.¹⁴

MATERIALS AND METHODS

Bacterial Strains, Plasmids, Materials, and Instrumentation. The chemically competent *Escherichia coli* TOP10 and BL21(DE3) strains were purchased from Invitrogen (Carlsbad, CA). The genomic DNA from *Msm* strain MC2 155 used for polymerase chain reaction (PCR) was a generous gift from S. Ehrt (Weill Cornell Medical College). The pET28a plasmid was purchased from Novagen (Gibbstown, NJ). All restriction enzymes, T4 DNA ligase, and Phusion DNA polymerase were purchased from NEB (Ipswich, MA). PCR primers were purchased from Integrated DNA Technologies (IDT, Coralville, IA). DNA sequencing was performed at the University of Michigan DNA Sequencing Core. Chemical reagents, including DTNB, AcCoA, AGs (APR, AMK, HYG, KAN, NEO, SIS, SPT, STR, and RIB) (Figure S2 of the Supporting Information), and chlorhexidine (1), were purchased from Sigma-Aldrich (Milwaukee, WI). The rest of the AGs (NEA, NET, PAR, and TOB) (Figure S2 of the Supporting Information) were purchased from AK Scientific (Mountain View, CA). Compound 2 was purchased from ChemDiv Inc. (San Diego, CA). The pH was adjusted at room temperature. The spectrophotometric assays were performed on a multi-mode SpectraMax M5 plate reader using 96-well plates (Fisher Scientific, Pittsburgh, PA). Silica gel 60 F₂₅₄ plates (Merck) were used for thin-layer chromatography (TLC) analysis. Liquid chromatography with mass spectrometry (LC–MS) was performed on a Shimadzu LCMS-2019EV instrument equipped with an SPD-20AV UV–vis detector and an LC-20AD liquid chromatography.

Preparation of the pEis-pET28a Overexpression Constructs. The pEis_Mtb-pET28a plasmid encoding the Eis_Mtb protein was constructed as previously reported.¹³ To prepare the pEis_Msm-pET28a construct, PCR was performed using *Msm* strain MC2 155 genomic DNA as a template, a forward primer 5'-TCGAGACATATGATCACGCCGCG-CACCCTTC-3', a reverse primer 5'-CCC GCGGGATCCT-CAGAATCCGTATCCCAGC-3', and Phusion DNA polymerase. The resulting amplified *eis_Msm* gene PCR fragment was inserted into the linearized pET28a plasmid via the corresponding *Nde*I and *Bam*HI restriction sites (underlined above). The plasmid encoding the Eis_Msm protein was transformed into *E. coli* TOP10 chemically competent cells. The plasmid bearing the *eis_Msm* gene insert was sequenced and showed perfect alignment with the reported gene sequence from *Msm* strain MC2 155 (locus tag MSMEG_3513).

Overproduction and Purification of Eis Proteins. The Eis_Mtb protein (with an N-terminal His₆ tag) was prepared as previously reported.¹³ The overexpression and purification of the Eis_Msm protein were performed exactly as reported for Eis_Mtb.¹³ Both proteins were dialyzed in Tris-HCl buffer (50 mM, pH 8.0) and stored at 4 °C. After purification, 1.1 mg of the 46172 Da Eis_Msm protein was obtained per liter of culture.

Determination of the AG Selectivity Profile of Eis_Msm by a Spectrophotometric Assay. The acetyltransferase activity of Eis_Msm was monitored by a UV–vis assay in which the free thiol group of CoA, generated by the Eis_Msm enzyme-catalyzed reaction, was allowed to react with DTNB to produce 2-nitro-5-thiobenzoate (NTB²⁻). The production of further ionized NTB²⁻ was monitored by the increase in absorbance at 412 nm ($\epsilon_{412} = 14150 \text{ M}^{-1} \text{ cm}^{-1}$). Reactions of mixtures (100 μL) containing AcCoA (0.5 mM, 5 equiv), AG (0.1 mM, 1 equiv), DTNB (1 mM), and Tris-HCl (50 mM, pH 8.0) were initiated by addition of Eis_Msm (0.5 μM) at 25 °C. Reactions were monitored by taking readings every 30 s for 15 min in a 96-well plate format.

Determination and Confirmation of the Number of Acetylation Sites by the Spectrophotometric Assay and Mass Spectrometry. To determine the number of acetylations performed by Eis_Msm for a given AG, we conducted two reactions with each AG: a calibration reaction with 1 equiv of AG and 1 equiv of AcCoA as well as a reaction

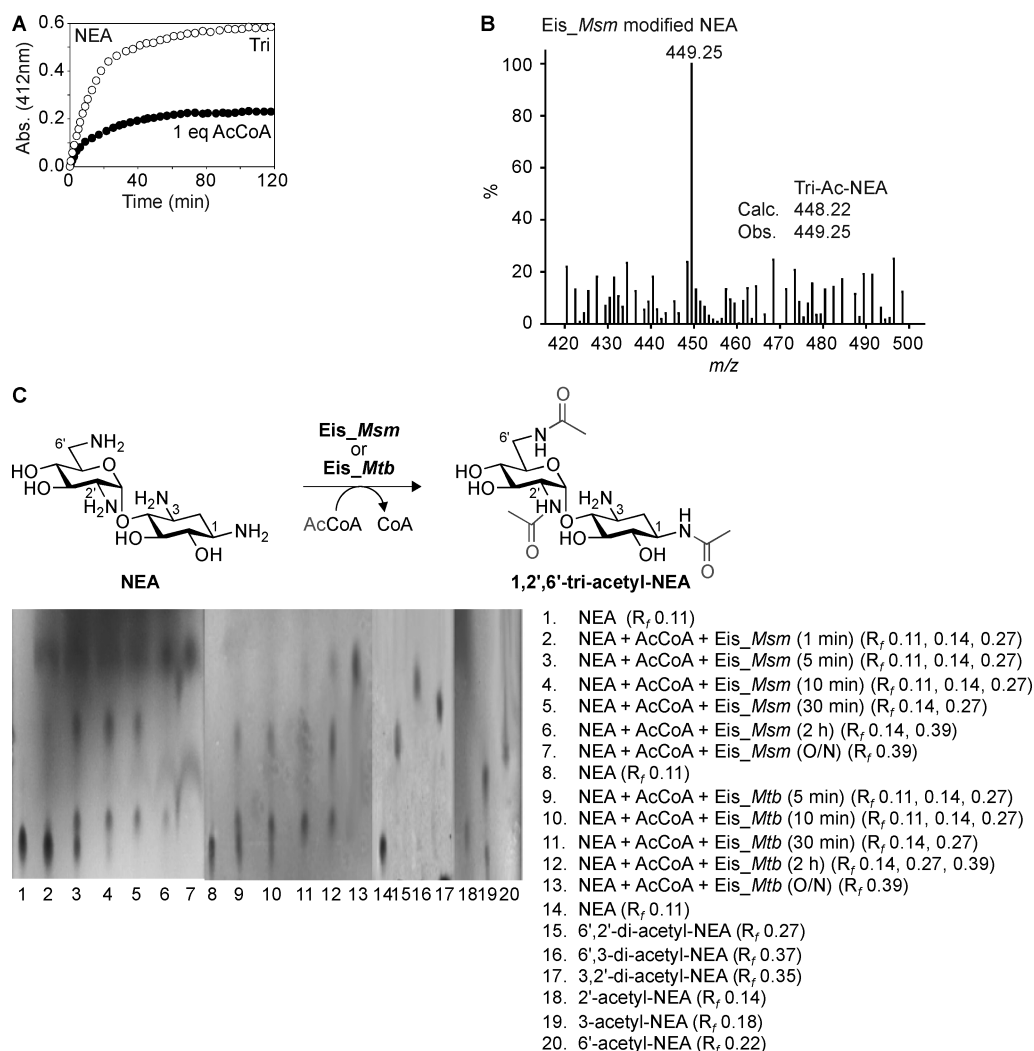


Figure 2. (A) Conversion of NEA into its acetylated products, as monitored by the UV–vis assay when using *Eis_Msm* with 1 (●) and 10 equiv (○) of AcCoA. (B) Mass spectrum confirming the formation of triacetyl-NEA by *Eis_Msm*. (C) Multiacetylation of NEA by *Eis_Msm* observed by the TLC assay. Lanes 1–7 show a time course displaying the mono-, di-, and triacetyl-NEA products of the *Eis_Msm* reaction. Lanes 8–13 show a time course of the NEA reaction with *Eis_Mtb*. Lanes 14–20 show controls for di- and monoacetylation of NEA performed with AAC(2')-Ic, AAC(3)-IV, and AAC(6') sequentially or individually.

that ensured complete acetylation of the AG with 1 equiv of AG and 10 equiv of AcCoA. Specifically, reactions of mixtures (100 μ L) containing AG (0.1 mM), DTNB (1 mM), Tris-HCl (50 mM, pH 8.0), and AcCoA (0.1 mM, 1 equiv, or 1 mM, 10 equiv) were initiated by addition of *Eis_Msm* (1 μ M) at 25 $^{\circ}$ C. Reactions were monitored at 412 nm as described above by taking readings every 30 s until a plateau was reached. Representative plots are shown in Figure 2A and Figure S3 of the Supporting Information. To confirm the number of acetylations on each AG substrate established by UV–vis assays, we conducted a third reaction with a mixture (20 μ L) containing AG (0.67 mM, 1 equiv), AcCoA (3.35 mM, 5 equiv), Tris-HCl (50 mM, pH 8.0), and *Eis_Msm* protein (10 μ M) overnight at 25 $^{\circ}$ C. These reactions were terminated by addition of an equal volume of ice-cold MeOH (20 μ L), which was then kept at -20 $^{\circ}$ C for at least 20 min. The precipitated protein was removed by centrifugation (13000 rpm at room temperature for 10 min). The masses of the acetylated AG products present in each sample were determined by LC–MS in positive mode using H₂O (0.1% formic acid) after dilution of the supernatant (10 μ L) with H₂O (20 μ L) and injection of all

30 μ L. Mass spectra of all AGs modified by *Eis_Msm* are provided in Figure 2B and Figure S4 of the Supporting Information. A summary of the level of acetylation is presented in Table 1.

Kinetic Characterization of *Eis_Msm* Activity. The steady-state kinetic assays of acetylation of AGs (AMK, KAN, NEA, NEO, NET, PAR, SIS, and TOB) by *Eis_Msm* were performed in two ways: (i) at a fixed concentration of AcCoA (0.1 mM) and varying concentrations of AGs (0, 31.25, 62.5, 125, 250, and 500 μ M) and (ii) at a fixed concentration of each AG (0.5 mM) and varying concentrations of AcCoA (0, 16.625, 31.25, 62.5, 125, and 250 μ M). All reactions were conducted in Tris-HCl (50 mM, pH 8.0), and all mixtures contained AcCoA, AG, DTNB (1 mM), and *Eis_Msm* (0.25 μ M). In addition, to distinguish among possible kinetic mechanisms, we conducted KAN acetylation reactions with *Eis_Msm* at AcCoA concentrations of 100, 200, and 500 μ M and for each of these concentrations at AG concentrations of 0, 20, 50, 100, 250, 500, 1000, and 2000 μ M. All reactions were initiated by addition of AcCoA and performed in at least duplicate at 25 $^{\circ}$ C. As described above, the acetylation reactions were monitored at

Table 1. Comparison of Levels of Acetylation by Eis from *M. smegmatis* and *M. tuberculosis*

AG	<i>M. smegmatis</i>	<i>M. tuberculosis</i> ^a
AMK	tri	tri
APR	di	× ^b
HYG	mono	di
KAN	di	di
NEA	tri	tri
NEO	tri	tri
NET	di	di
PAR	tri	di
RIB	tri	tri
SIS	tri	tri
SPT	× ^b	× ^b
STR	× ^b	× ^b
TOB	tetra	tetra

^aWe previously reported these data.¹³ ^bNo acetylation observed.

412 nm as a function of time, and absorbance readings were taken every 20 s. The dependence of the initial rates on the concentration of a titrant was used to calculate the apparent Michaelis–Menten kinetic parameters, $K_{m,AG}$ and $k_{cat,AG}$ (for reactions of type i above) as well as $K_{m,AcCoA}$ and $k_{cat,AcCoA}$ (for reactions of type ii), by nonlinear least-squares regression data fitting with SigmaPlot (Systat Software, San Jose, CA) to the Michaelis–Menten equation. These kinetic parameters are listed in Tables 2 and 3.

Table 2. Observed Kinetic Parameters^a for AG Concentration-Dependent Acetylation by Eis from *M. smegmatis* and *M. tuberculosis*

AG	<i>M. smegmatis</i>		<i>M. tuberculosis</i>	
	$K_{m,AG}$ (μM)	$k_{cat,AG}$ (s ⁻¹)	$K_{m,AG}$ (μM)	$k_{cat,AG}$ (s ⁻¹)
AMK	251 ± 55	0.034 ± 0.003	113 ± 35	0.030 ± 0.004
KAN	278 ± 36	0.108 ± 0.005	490 ± 140	0.12 ± 0.02
NEA	359 ± 101	0.176 ± 0.027	137 ± 57	0.064 ± 0.010
NEO	314 ± 77	0.114 ± 0.014	199 ± 87	0.19 ± 0.04
NET	197 ± 30	0.835 ± 0.057	96 ± 15	0.63 ± 0.03
PAR	153 ± 55	0.035 ± 0.006	96 ± 20	0.15 ± 0.01
SIS	82 ± 8	0.206 ± 0.006	159 ± 48	0.38 ± 0.04
TOB	131 ± 22	0.267 ± 0.016	116 ± 17	0.21 ± 0.01

^aAll parameters are defined in Materials and Methods.

Table 3. Observed Kinetic Parameters^a for AcCoA Concentration-Dependent Acetylation by Eis from *M. smegmatis* and *M. tuberculosis*

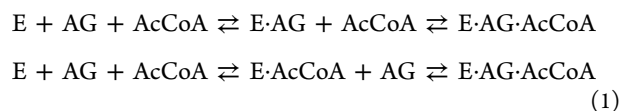
AG	<i>M. smegmatis</i>		<i>M. tuberculosis</i>	
	$K_{m,AcCoA}$ (μM)	$k_{cat,AcCoA}$ (s ⁻¹)	$K_{m,AcCoA}$ (μM)	$k_{cat,AcCoA}$ (s ⁻¹)
AMK	58 ± 25	0.142 ± 0.026	8 ± 5	0.015 ± 0.001
KAN	39 ± 17	0.398 ± 0.060	10 ± 3	0.094 ± 0.004
NEA	22 ± 7	0.101 ± 0.008	41 ± 6	0.070 ± 0.004
NEO	76 ± 23	0.546 ± 0.065	32 ± 6	0.116 ± 0.005
NET	108 ± 35	0.819 ± 0.121	124 ± 23	0.36 ± 0.03
SIS	77 ± 19	0.620 ± 0.063	84 ± 11	0.90 ± 0.04

^aAll parameters are defined in Materials and Methods.

To convert these observed kinetic parameters into the mechanistic rate constants, we considered three mechanisms: (1) the random sequential mechanism, in which either AcCoA

or AG can bind to the free enzyme followed by binding of the other species, (2) the ordered sequential mechanism, in which AcCoA binds Eis first, followed by AG, and (3) the ordered sequential mechanism, in which AG binds Eis first, followed by AcCoA.

The random sequential mechanism is described by the following kinetic steps:



where E is the enzyme and AG-Ac is the acetylated AG product.

Under the common simplifying assumptions of rapid AcCoA and AG binding equilibria for this mechanism, one obtains the observed kinetic parameters defined above in terms of microscopic constants:

$$k_{cat,AG} = \frac{k_{cat}[AcCoA]}{K_{d,AcCoA}(E \cdot AG) + [AcCoA]} \quad (2)$$

$$K_{m,AG} = K_{d,AG}(E \cdot AcCoA) \left[\frac{K_{d,AcCoA}(E) + [AcCoA]}{K_{d,AcCoA}(E \cdot AG) + [AcCoA]} \right] \quad (3)$$

$$k_{cat,AcCoA} = \frac{k_{cat}[AG]}{K_{d,AG}(E \cdot AcCoA) + [AG]} \quad (4)$$

$$K_{m,AcCoA} = K_{d,AcCoA}(E \cdot AG) \left[\frac{K_{d,AG}(E) + [AG]}{K_{d,AG}(E \cdot AcCoA) + [AG]} \right] \quad (5)$$

where each subscript of an equilibrium binding constant K_d designates the step in mechanism 1; the species outside of the parentheses binds to the species in the parentheses, and k_{cat} is the microscopic rate constant of acetylation, i.e., the last step in mechanism 1.

The ordered sequential mechanism, in which only AcCoA can bind Eis, is obtained by removing the first line in mechanism 1. For this mechanism, under the assumption of rapid equilibria, one obtains

$$k_{cat,AG} = k_{cat} \quad (6)$$

$$K_{m,AG} = K_{d,AG} \left(1 + \frac{K_{d,AcCoA}}{[AcCoA]} \right) \quad (7)$$

$$k_{cat,AcCoA} = \frac{k_{cat}[AG]}{K_{d,AG} + [AG]} \quad (8)$$

$$K_{m,AcCoA} = \frac{K_{d,AcCoA}K_{d,AG}}{K_{d,AG} + [AG]} \quad (9)$$

For the other ordered sequential mechanism, in which AG binds Eis first, we obtain by analogy

$$k_{cat,AG} = \frac{k_{cat}[AcCoA]}{K_{d,AcCoA} + [AcCoA]} \quad (10)$$

$$K_{m,AG} = \frac{K_{d,AG}K_{d,AcCoA}}{K_{d,AcCoA} + [AcCoA]} \quad (11)$$

$$k_{\text{cat,AcCoA}} = k_{\text{cat}} \quad (12)$$

$$K_{\text{m,AcCoA}} = K_{\text{d,AcCoA}} \left(1 + \frac{K_{\text{d,AG}}}{[\text{AG}]} \right) \quad (13)$$

The different functional dependencies of the observed Michaelis–Menten parameters on the concentrations of AG and AcCoA for the three mechanisms allow one to distinguish among them.

For the random sequential mechanism, eqs 2–4 yield

$$\frac{k_{\text{cat,AG}}}{K_{\text{m,AG}}k_{\text{cat,AcCoA}}} = \frac{[\text{AcCoA}]}{[\text{AG}]} \left[\frac{1}{K_{\text{d,AcCoA}}(\text{E}) + [\text{AcCoA}]} \right] \left[\frac{K_{\text{d,AG}}(\text{E} \cdot \text{AcCoA}) + [\text{AG}]}{K_{\text{d,AG}}(\text{E} \cdot \text{AcCoA})} \right] \quad (14)$$

The left-hand side of the equality is composed of observed constants. The expression in the first parentheses on the right-hand side of the equality is constant for all AGs and, by an assumption, similar for the two Eis proteins, as explained in Results. This allows one to obtain an estimate of $K_{\text{d,AG}}(\text{E} \cdot \text{AcCoA})$ followed by the determination of the k_{cat} from eq 4. These values are listed in Table 5. Where only bounds on these values could be obtained because of a very low affinity of an AG for AcCoA-bound Eis [$K_{\text{d,AG}}(\text{E} \cdot \text{AcCoA}) \gg [\text{AG}]$], only the catalytic efficiency [$k_{\text{cat}}/K_{\text{d,AG}}(\text{E} \cdot \text{AcCoA})$] was calculated from eq 4 and reported.

Determination of Positions Acetylated on NEA by Eis_{Msm} by TLC. To establish which three positions of the NEA scaffold are acetylated by Eis_{Msm}, reactions (40 μL) were conducted at room temperature in Tris-HCl buffer (50 mM, pH 8.0) in the presence of AcCoA (4 mM, 5 equiv), NEA (0.8 mM, 1 equiv), and Eis_{Msm} (5 μM). Aliquots (4 μL) were loaded and run on a TLC plate after 0, 1, 5, 10, 30, and 120 min as well as after overnight incubation (Figure 2C). The eluent system utilized for the TLC was a 3:0.8 MeOH/NH₄OH mixture. Visualization was achieved using a cerium–molybdate stain (5 g of cerium ammonium nitrate, 120 g of ammonium molybdate, 80 mL of H₂SO₄, and 720 mL of H₂O). The R_f values of the Eis_{Msm}-modified NEA were consistent with those obtained for the reaction of Eis_{Mtb} with NEA (Figure 2C).¹³ Control reactions for mono- and diacetylation of NEA were performed using the AG acetyltransferases AAC(2')-Ic from *M. tuberculosis* H37Rv,¹³ AAC(3)-IV from *E. coli*,¹⁵ and AAC(6') from the AAC(6')/APH(2'') bifunctional enzyme individually and sequentially.¹⁵

Determination of Kinetic Parameters and Mode of Inhibition for Inhibitors of Eis_{Msm}. The IC₅₀ values of two inhibitors, chlorhexidine (1) and compound 2, were determined as previously described.¹⁴ Briefly, the inhibitors were dissolved in Tris-HCl [50 mM, pH 8.0, containing 10% (v/v) DMSO] (100 μL), and 5-fold dilution series were performed. To these solutions was added a mixture (50 μL) containing Eis (1 μM), NEO (400 μM), and Tris-HCl (50 mM, pH 8.0), and the solutions were incubated at room temperature for 10 min. The reactions were initiated by addition of a mixture (50 μL) containing AcCoA (2 mM; ensuring that all Eis is in the AcCoA-bound form), DTNB (2 mM), and Tris-HCl (50 mM, pH 8.0). The absorbance change at 412 nm was monitored every 30 s for 15 min at 25 °C. Initial rates were calculated, and the IC₅₀ values were determined by using a Hill

plot analysis by using KaleidaGraph version 4.1 (Synergy software, Reading, PA) (Figure 3).

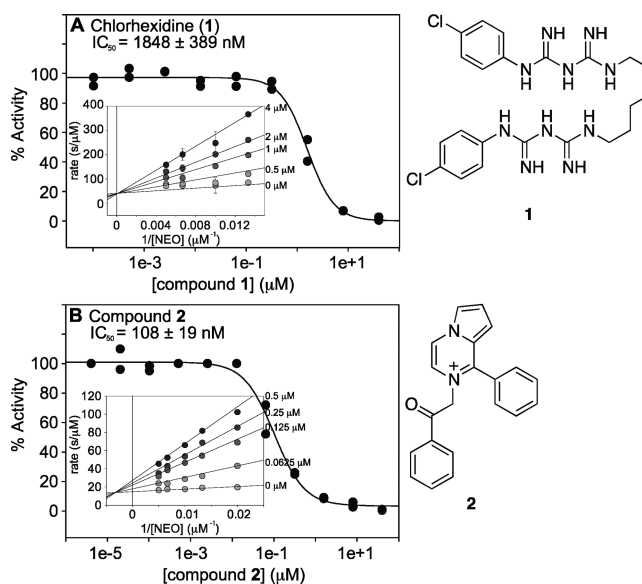


Figure 3. Inhibition of Eis_{Msm}. IC₅₀ curves for (A) chlorhexidine (1) and (B) compound 2. The insets show the competitive and mixed inhibition modes of compounds 1 and 2, respectively.

To determine the mode of inhibition of both compounds tested, we used varying concentrations of NEO (final concentrations of 50, 75, 100, 150, and 200 μM) and chlorhexidine (1) (final concentrations of 0, 0.5, 1, 2, and 4 μM) or compound 2 (final concentrations of 0, 0.0625, 0.125, 0.25, and 0.5 μM). Chlorhexidine (1) was found to be a competitive inhibitor of NEO, whereas mixed inhibition was observed for compound 2. The equilibrium constants (K_i) for binding of chlorhexidine (1) to the Eis-AcCoA complex and constants K_i and K_i' for binding of compound (2) to the Eis-AcCoA and Eis-AcCoA-AG complexes, respectively, were determined from the nonlinear least-squares regression fitting of data with SigmaPlot to a Michaelis–Menten equation:

$$V = \frac{(1/\alpha')V_{\text{max,AG}}[\text{AG}]}{(\alpha/\alpha')K_{\text{m,AG}} + [\text{AG}]} \quad (15)$$

where V is the steady-state reaction rate, $\alpha = 1 + [\text{I}]/K_i$, $\alpha' = 1 + [\text{I}]/K_i'$ ($\alpha' = 0$ for chlorhexidine), and $V_{\text{max,AG}}$ and $K_{\text{m,AG}}$ are the observed kinetic parameters for the reaction in the absence of inhibitor. The reaction rates are shown as Lineweaver–Burk plots (Figure 3, insets of panels A and B).

RESULTS

Substrate Specificity and Multiacetylation Profiles of Eis Proteins. Recently, we reported the structural and biochemical characterization of Eis_{Mtb}, an AG acetyltransferase (AAC) responsible for resistance to KAN in *Mtb* clinical isolates.¹³ We discovered Eis to be a novel AAC capable of unprecedented multiacetylation of a large number of AG scaffolds. In this study, to gain insight into the unique recognition and specificity rules for the N-acetylation by Eis proteins, we performed a detailed characterization of AG acetylation by Eis_{Msm}, a homologue of Eis_{Mtb}, and compared its functional properties to those of Eis_{Mtb}. To ensure the validity of the comparison, we identically cloned and

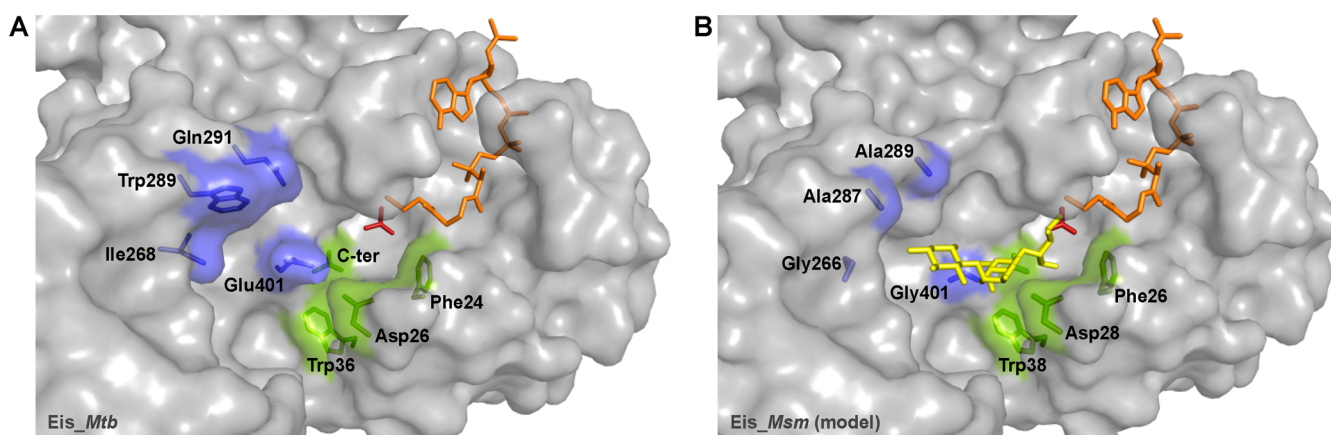


Figure 4. Structural differences between the AG-binding pockets of *Eis_Mtb* and *Eis_Msm*. (A) Active site and AG-binding pocket of *Eis_Mtb* bound to CoA and an acetamide, as seen in the recently reported crystal structure [Protein Data Bank (PDB) entry 3R1K¹³]. In both panels, CoA is colored orange, acetamide is colored red, the conserved AG-binding pocket residues are colored green, and the nonconserved residues are colored blue. The C-terminal carboxyl group is denoted as C-ter. (B) Model of the active site and the AG-binding pocket of *Eis_Msm*. This model was generated by substituting the nonconserved residues of the AG-binding pocket *Eis_Mtb* with their counterparts in *Eis_Msm* (Ile268, Trp289, and Gln291 in *Eis_Mtb* were mutated to Gly266, Ala287, and Ala289, respectively, in *Eis_Msm*). As a result of these mutations, an APR molecule (yellow) can be accommodated in the pocket in the orientation appropriate for catalysis. The structure of APR was taken from high-resolution PDB entry 2OE5.²⁷

heterologously expressed the 46172 Da *Eis_Msm* and the 46597 Da *Eis_Mtb* in *E. coli* as N-terminally His₆-tagged proteins. We first investigated the substrate specificity and the multiacetylation profile of *Eis_Msm* by spectrophotometric assays (Table 1, Figure 2A, and Figure S3 of the Supporting Information) and mass spectrometry (Figure 2B and Figure S4 of the Supporting Information). The data indicated that AMK, APR, HYG, KAN, NEA, NEO, NET, PAR, RIB, SIS, and TOB were substrates of *Eis_Msm*, whereas SPT and STR were not. We found *Eis_Mtb* and *Eis_Msm* to have generally similar AG substrate selectivity and N-acetylation profiles with SPT and STR not modified, KAN and NET diacetylated, AMK, NEA, NEO, RIB, and SIS triacetylated, and TOB tetra-acetylated by both *Eis* proteins. Interestingly, we observed three major differences in the activity of these two *Eis* proteins. (i) *Eis_Msm* diacetylated APR, an AG with conformationally restricted and extended cylindrical-like structure (Figure 4 and Figure S2 of the Supporting Information),^{16,17} which *Eis_Mtb* could not chemically modify. (ii) *Eis_Msm* triacetylated PAR, which could only be diacetylated by *Eis_Mtb*. (iii) *Eis_Msm* monoacetylated HYG, a structurally unique AG that could be diacetylated by *Eis_Mtb*. The identity of several nonconserved amino acid residues lining the AG-binding pocket of the two *Eis* proteins (highlighted in dark blue in Figures 1 and 4) is likely responsible for these differences in the number of acetylation sites.

Regiospecificity of Triacetylation of NEA by *Eis* Proteins. Knowing that the substrate profile for both *Eis* proteins was generally similar, we sought to compare the regiospecificity of their acetylating activity on an AG scaffold for which the number of sites acetylated was observed to be the same for the two proteins. We recently established by TLC and NMR spectroscopy that *Eis_Mtb* triacetylates NEA first at position 2', then at position 6', and finally at position 1.¹³ Here, by using TLC and comparing the retention factor (*R_f*) values of the mono-, di-, and triacetylated NEA derivatives produced over time by *Eis_Msm* to the *R_f* values of their counterparts formed by *Eis_Mtb* as well as to those of mono- and diacetylated NEA standards obtained by using individually or

sequentially monoacetylating AAC enzymes, we observed that *Eis_Msm* is also a 2',6',1-NEA-triacetylating enzyme (Figure 2C). These results suggest that AG scaffolds with the same number of acetylations by *Eis_Mtb* and *Eis_Msm* are likely modified by these two enzymes at the same positions.

Steady-State Kinetic Analysis of *Eis* Proteins. Seeking a deeper understanding of the subtleties differentiating *Eis_Mtb* and *Eis_Msm*, we determined the observed Michaelis–Menten catalytic parameters of steady-state acetylation for several AGs. We conducted two sets of reactions, one at a fixed concentration of AcCoA and varying concentrations of AGs (Table 2) and the other at a fixed concentration of each AG and varying concentrations of AcCoA (Table 3). To convert the observed kinetic parameters into the mechanistic rate constants, we considered three kinetic mechanisms of *Eis* acetylation: (1) the random sequential mechanism, in which either AcCoA or AG can bind to the free enzyme followed by binding of the other species, most commonly observed for other AAC enzymes,^{18–22} (2) the ordered sequential mechanism, in which AcCoA binds *Eis* only before AG does, observed for some AAC enzymes,^{23–25} and (3) the ordered sequential mechanism, in which AG binds *Eis* only before AcCoA does, not observed previously for other AAC enzymes.

To distinguish among these three mechanisms, we conducted steady-state kinetic measurements of acetylation of KAN by *Eis_Msm* at several AcCoA concentrations and for each AcCoA concentration at several KAN concentrations. For each AcCoA concentration, we obtained the AcCoA concentration-dependent observed Michaelis–Menten parameters *K_{m,AG}* and *k_{cat,AG}* (Table 4). Each of the three mechanisms of interest is characterized by a unique dependence of these

Table 4. Observed Kinetic Parameters for KAN Acetylation by *Eis* from *M. smegmatis*

[AcCoA] (μM)	<i>K_{m,AG}</i> (μM)	<i>k_{cat,AG}</i> (s ^{−1})
100	278 ± 36	0.108 ± 0.005
200	450 ± 31	0.18 ± 0.01
500	756 ± 66	0.40 ± 0.02

Table 5. Rate and Equilibrium Binding Constants^a for the Random Sequential Mechanism of Acetylation by Eis from *M. smegmatis* and *M. tuberculosis*

AG	<i>M. smegmatis</i>			<i>M. tuberculosis</i>			
	$K_{d,AG(E-AcCoA)}$ (μ M)	k_{cat} (s^{-1})	$k_{cat}/K_{d,AG(E-AcCoA)}$ ($s^{-1} M^{-1}$)	$K_{d,AG(E-AcCoA)}$ (μ M)	k_{cat} (s^{-1})	$k_{cat}/K_{d,AG(E-AcCoA)}$ ($s^{-1} M^{-1}$)	$K_{d,AcCoA(E)}$ (μ M) ^b
AMK	>1000	>0.3	284 \pm 52	32 \pm 14	0.016 \pm 0.007	500 \pm 300	87 \pm 23
KAN	2540 \pm 160	1.6 \pm 0.5	630 \pm 200	350 \pm 150	0.16 \pm 0.07	460 \pm 280	
NEA	141 \pm 60	0.13 \pm 0.05	917 \pm 500	95 \pm 50	0.08 \pm 0.04	870 \pm 640	
NEO	>1000	>1.0	1090 \pm 130	75 \pm 41	0.13 \pm 0.07	1800 \pm 1400	
NET	108 \pm 35	1.0 \pm 0.4	7900 \pm 4000	31 \pm 10	0.4 \pm 0.1	12200 \pm 5600	
SIS	179 \pm 54	0.85 \pm 0.25	4700 \pm 2050	340 \pm 140	1.5 \pm 0.6	4500 \pm 2600	

^aAll parameters are defined in Materials and Methods. Determination of the rest of the equilibrium constants of the mechanism by this method was not reliable because of large propagated uncertainties. ^bThis value is AG-independent and assumed to be the same for Eis_Msm and Eis_Mtb (see the text) in the calculations of the Eis_Mtb parameters in this table.

kinetic parameters on the concentration of AcCoA, as described in Materials and Methods. Notably, the random sequential mechanism is the only one of the three mechanisms for which $K_{m,AG}$ can increase with an increasing AcCoA concentration [for $K_{d,AcCoA(E)} < K_{d,AcCoA(E-AG)}$ in eq 3], which is what we observe (Table 4). Therefore, either ordered mechanism is inconsistent with the data. Furthermore, the dependencies of $k_{cat,AG}$ and $K_{m,AG}$ on AcCoA concentration agree with the random sequential mechanism described by eqs 2 and 3. Fitting the data to these two equations yields the microscopic mechanistic constants: $k_{cat} = 1.6 \pm 0.5 s^{-1}$, $K_{d,AcCoA(E-AG)} = 1460 \pm 600 \mu$ M, $K_{d,AG(E-AcCoA)} = 2540 \pm 160 \mu$ M, and $K_{d,AcCoA(E)} = 87 \pm 23 \mu$ M. Indeed, consistent with the qualitative assessments described above, $K_{d,AcCoA(E)}$ is approximately 17-fold smaller than $K_{d,AcCoA(E-AG)}$. The equilibrium binding constant for binding of AcCoA to the free Eis protein [$K_{d,AcCoA(E)}$] is independent of the nature of an AG molecule. Moreover, because all the AcCoA binding residues are identical in Eis_Msm and Eis_Mtb (Figure 1), it is reasonable to assume the same value of $K_{d,AcCoA(E)}$ for both enzymes. This allows us to obtain microscopic constants k_{cat} and $K_{d,AG(E-AcCoA)}$ or their ratio for Eis_Msm and Eis_Mtb from the data in Tables 2 and 3, as explained in Materials and Methods (Table 5).

These values indicate that generally AG binds the complex of Eis with AcCoA more weakly for Msm than for Mtb. Interestingly, this weaker binding is compensated by faster catalytic rate constants (k_{cat}), which result in comparable catalytic efficiencies [$k_{cat}/K_{d,AG(E-AcCoA)}$] for the two proteins, irrespective of the nature of an AG substrate. For the two AGs used against Mtb in the clinic, KAN and AMK, this effect appears to be most dramatic; they bind the Eis_Mtb-AcCoA complex with much higher affinity than the Eis_Msm complex but display much higher k_{cat} values with Eis_Msm. Catalytic efficiencies varied over a 10–20-fold range among different AG substrates. For both Eis proteins, NET and SIS displayed the highest catalytic efficiencies among the AGs. For these two AGs, the AG affinity and k_{cat} values were similar for the two Eis homologues.

Inhibition of Eis Proteins. To further probe the differences in the active sites of Eis_Mtb and Eis_Msm, we next investigated with Eis_Msm the activity of the two inhibitors, chlorhexidine (1) and compound 2, that we recently identified from a high-throughput screening study with Eis_Mtb (Figure 3).¹⁴ We previously showed that these two Eis inhibitors display high selectivity toward the Eis_Mtb AG-binding site over that of any other types of AAC enzymes. Here, we found both inhibitors of Eis_Mtb to be effective against Eis_Msm in an analogous NEO acetylation assay.

Interestingly, with an IC_{50} value of 1848 ± 389 nM, chlorhexidine (1) appeared to be a 10-fold worse inhibitor of Eis_Msm than of Eis_Mtb ($IC_{50} = 188 \pm 30$ nM). In contrast, with an IC_{50} value of 108 ± 19 nM, compound 2 appeared to be a 3-fold better inhibitor of Eis_Msm than of Eis_Mtb ($IC_{50} = 364 \pm 32$ nM). Consistently with the previously reported mode of inhibition for Eis_Mtb,¹⁴ we observed that compounds 1 and 2 displayed the AG-competitive mode and the mixed mode of inhibition against NEO, respectively, when tested against Eis_Msm. The Michaelis–Menten analysis of the inhibition kinetics for compound 1 yields K_i values of 470 ± 150 nM for Eis_Msm and 105 ± 24 nM for Eis_Mtb, where K_i is the affinity of the inhibitor for the Eis-AcCoA complex. For compound 2, which displays the mixed inhibition mode, K_i and K_i' values are 990 ± 520 and 320 ± 170 nM for Eis_Msm and 203 ± 47 and 547 ± 19 nM for Eis_Mtb, respectively, where K_i' is the affinity of the inhibitor for the Eis-AcCoA-AG ternary complex. Thus, this compound binds with comparable affinities to the Eis-AcCoA-AG ternary complex and to the Eis-AcCoA binary complex, for both Eis_Msm and Eis_Mtb (for either Eis protein), indicating that it does not bind directly in the AG-binding site. These results demonstrate the potential of inhibitors of Eis_Mtb for use against other mycobacterial species.

DISCUSSION

Eis is an Mtb protein whose upregulation leads to KAN resistance, a hallmark of XDR-TB, in a large set of clinical isolates from different regions of the world.¹¹ With its hexameric structure and its AG multiacetylating capabilities, Eis_Mtb is an AAC that is structurally and functionally highly divergent from all other characterized AACs.¹³ Eis homologues are found in a number of pathogenic and nonpathogenic mycobacteria, including Mtb and Msm (Figure 1 and Figure S1 of the Supporting Information). The low level of sequence identity (10%) among Eis homologues from 10 mycobacteria presented in Figure S1 of the Supporting Information may prompt one to assume that substrate recognition rules used by Eis_Mtb may not apply to other mycobacteria. Upon closer inspection of these sequence alignments, we find that the amino acid residues involved in CoA and AG binding as well as in catalysis are highly or even strictly conserved. Therefore, we can hypothesize that the discoveries made and information gained for Eis_Mtb may find application to other diseases of mycobacterial origin. In fact, the generally minor variation of the putative AG-interacting residues sets up different mycobacteria as good systems for studying the poorly understood AG-recognition rules of Eis. For several decades,

Msm has been used as a model system to study mechanisms of *Mtb*. The sequences of *Eis_Msm* and *Eis_Mtb* are 58% identical (Figure 1). All amino acid residues involved in CoA binding and catalysis are strictly conserved between *Eis_Msm* and *Eis_Mtb*. However, there are four amino acid residues (highlighted in dark blue in Figures 1 and 4) in the AG-binding pockets of these two proteins that differ.

In this work, we have focused on improving our understanding of the evolution of the novel multiacetylation mechanism of *Eis* and on probing the potential application of novel *Eis_Mtb* inhibitors against other mycobacterial organisms. Our steady-state kinetic measurements indicated that *Eis_Msm*, like *Eis_Mtb*, is able to efficiently multiacetylate many AGs and that it employs the random sequential mechanism of acetylation, like the majority of the other mechanistically characterized AACs.^{18–22} Interestingly, the binding affinities and the catalytic rate constants differed between the two enzymes for most AGs, whereas the catalytic efficiencies were very similar. Structurally, very similar NET and SIS were acetylated with the highest efficiencies among AGs for both proteins and display comparable kinetic properties. This suggests that these two AGs must interact mostly with the features of the binding pockets that are conserved between the two enzymes. Despite the overall similarities between *Eis_Msm* and *Eis_Mtb*, we observed a major variation in the acetylating activity of APR by these two enzymes. *Eis_Msm* diacetylated APR, whereas *Eis_Mtb* did not accept APR as a substrate. APR is a structurally unique AG that contains four rings, with the two central rings fused (Figure S1 of the Supporting Information). This chemical structure limits the conformational freedom of this molecule, and as a result, APR has an extended cylinder-like conformation, as observed both in a crystalline form¹⁶ and in solution.¹⁷ Furthermore, this extended conformation of APR is essentially unchanged in several crystal structures of APR bound to RNA ligands.^{26–28} Therefore, the AG-binding cavity of an enzyme needs to be sufficiently wide and long to accommodate a bound APR molecule for its acetylation. Because *Eis_Mtb* is unable to acetylate APR and *Eis_Msm* acetylates APR at two positions, the stiff APR scaffold serves as an excellent AG specificity discriminator between the two homologues. To explain this major specificity difference, we looked for structural features that could allow *Eis_Msm* to accommodate an APR molecule in the *Eis_Msm*, but not in the *Eis_Mtb* binding site. Because three of the four primary amines of APR lie on the “terminal” rings, at least one of them is modified, which means that the AG-binding pocket should be wide and long enough to accommodate an APR cylinder with one end of it placed at the active site.

As seen in the crystal structure of *Eis_Mtb* in complex with CoA and an acetamide determined recently by our group,¹³ the AG-binding cavity of *Eis_Mtb* is bifurcated, with Glu401 separating the cavity into two channels (with borders highlighted in green and blue in Figure 4A). One channel (green) is not straight enough to fit an APR molecule without steric clashes in both *Eis_Mtb* and *Eis_Msm*. Most residues lining this channel are the same in *Eis_Mtb* and *Eis_Msm* (in *Eis_Msm* numbering in Figure 1, Phe26, Asp28, and Trp38, and the carboxyl terminus denoted C-ter in Figure 4). In particular, it is not possible to prevent clashes between the APR and the catalytic carboxyl terminus, whose position is likely highly conserved,¹³ and with Trp38 (Trp36 in *Eis_Mtb*). The other channel (blue) is fairly shallow in *Eis_Mtb* because of Glu401. In addition, this channel is capped at the end by

Trp289 and Ile268 in *Eis_Mtb*, imposing additional steric restrictions on the length of the ligand. Interestingly, all differences in the AG-binding pockets of *Eis_Mtb* and *Eis_Msm* lie in the residues that line this channel. Moreover, in *Eis_Msm*, the residues in this channel are smaller than those in *Eis_Mtb*, thus likely resulting in a longer and wider channel in *Eis_Msm* than in *Eis_Mtb* and creating a cavity large enough to bind an APR molecule in a proper orientation for acetylation (Figure 4B). Specifically, Trp289 in *Eis_Mtb* is changed to an alanine (Ala287 in *Eis_Msm*), and Ile268 and Glu401 in *Eis_Mtb* are changed to glycines (Gly266 and Gly401 in *Eis_Msm*, respectively) (Figures 1 and 4). In addition, another residue lining this channel, Gln291 in *Eis_Mtb* is replaced with a smaller alanine (Ala289 in *Eis_Msm*), contributing to the channel widening. An APR molecule readily fits into this channel in the model of an *Eis_Msm* structure (Figure 4B). Even though the structural details of binding of APR to *Eis_Msm* may not all be accurately represented by this model, when taken together, our biochemical results and these structural considerations suggest that APR binding occurs in this channel.

Finally, by demonstrating that inhibitors of *Eis_Mtb* can also prevent acetylation of NEO by *Eis_Msm*, we showed that the *Eis_Mtb* inhibitory properties of these compounds could potentially be extended to other mycobacteria. As we demonstrated, the inhibitory power of each compound was somewhat different between the two mycobacteria, suggesting that these inhibitors would display varying potencies among mycobacteria. Further investigations are currently underway in our laboratory to determine appropriate inhibitor–mycobacterium pairs. In the future, testing the activity of these inhibitors against other *Eis*-containing pathogenic bacteria to evaluate the extent of the application of these molecules will be of interest.

■ ASSOCIATED CONTENT

● Supporting Information

Figures showing the multiple-sequence alignment of *Eis* homologues from a variety of mycobacteria, structures of the *Eis_Msm* AG substrates, representative UV–vis plots monitoring the conversion of various AGs to their acetylated products with 1 and 10 equiv of AcCoA, and mass spectra of the AGs acetylated by *Eis_Msm*. This material is available free of charge via the Internet at <http://pubs.acs.org>.

■ AUTHOR INFORMATION

Corresponding Author

*E-mail: sylviegt@umich.edu. Phone: (734) 615-2736. Fax: (734) 615-5521.

Funding

Funding support for this work was provided by the Life Sciences Institute (S.G.-T.) and the College of Pharmacy at the University of Michigan (S.G.-T. and O.V.T.), National Institutes of Health Grant AI090048 (S.G.-T.), and a grant from the Firland Foundation (S.G.-T.).

Notes

The authors declare no competing financial interest.

■ ACKNOWLEDGMENTS

We thank Prof. Sabine Ehrt (Weill Cornell Medical College) for the gift of the *M. smegmatis* strain MC2 155 genomic DNA.

■ ABBREVIATIONS

AcCoA, acetyl-coenzyme A; AMK, amikacin; AG, aminoglycoside; AAC, aminoglycoside acetyltransferase; APH, aminoglycoside phosphotransferase; APR, apramycin; DTNB, 5,5'-dithiobis(2-nitrobenzoic acid); Eis, enhanced intracellular survival; HYG, hygromycin; KAN, kanamycin A; LC-MS, liquid chromatography with mass spectrometry; *Msm*, *M. smegmatis*; *Mtb*, *M. tuberculosis*; NEA, neamine; NEO, neomycin B; NET, netilmicin; PAR, paromomycin; RIB, ribostamycin; SIS, sisomicin; SPT, spectinomycin; STR, streptomycin; TLC, thin-layer chromatography; TOB, tobramycin; TB, tuberculosis.

■ REFERENCES

- (1) Caminero, J. A. (2006) Treatment of multidrug-resistant tuberculosis: Evidence and controversies. *Int. J. Tuberc. Lung Dis.* 10, 829–837.
- (2) Chan, E. D., Laurel, V., Strand, M. J., Chan, J. F., Huynh, M. L., Goble, M., and Iseman, M. D. (2004) Treatment and outcome analysis of 205 patients with multidrug-resistant tuberculosis. *Am. J. Respir. Crit. Care Med.* 169, 1103–1109.
- (3) Ellner, J. J. (2008) The emergence of extensively drug-resistant tuberculosis: A global health crisis requiring new interventions: Part I: The origins and nature of the problem. *Clin. Transl. Sci.* 1, 249–254.
- (4) Banerjee, R., Schechter, G. F., Flood, J., and Porco, T. C. (2008) Extensively drug-resistant tuberculosis: New strains, new challenges. *Expert Rev. Anti-Infect. Ther.* 6, 713–724.
- (5) Udawadia, Z. F., Amale, R. A., Ajani, K. K., and Rodrigues, C. (2012) Totally drug-resistant tuberculosis in India. *Clin. Infect. Dis.* 54, 579–581.
- (6) Shiloh, M. U., and DiGiuseppe Champion, P. A. (2010) To catch a killer. What can mycobacterial models teach us about *Mycobacterium tuberculosis* pathogenesis? *Curr. Opin. Microbiol.* 13, 86–92.
- (7) Reyrat, J. M., and Kahn, D. (2001) *Mycobacterium smegmatis*: An absurd model for tuberculosis? *Trends Microbiol.* 9, 472–474.
- (8) Tyagi, J. S., and Sharma, D. (2002) *Mycobacterium smegmatis* and tuberculosis. *Trends Microbiol.* 10, 68–69.
- (9) Cole, S. T., Brosch, R., Parkhill, J., Garnier, T., Churcher, C., Harris, D., Gordon, S. V., Eiglmeier, K., Gas, S., Barry, C. E., III, Tekaia, F., Badcock, K., Basham, D., Brown, D., Chillingworth, T., Connor, R., Davies, R., Devlin, K., Feltwell, T., Gentles, S., Hamlin, N., Holroyd, S., Hornsby, T., Jagels, K., Krogh, A., McLean, J., Moule, S., Murphy, L., Oliver, K., Osborne, J., Quail, M. A., Rajandream, M. A., Rogers, J., Rutter, S., Seeger, K., Skelton, J., Squares, R., Squares, S., Sulston, J. E., Taylor, K., Whitehead, S., and Barrell, B. G. (1998) Deciphering the biology of *Mycobacterium tuberculosis* from the complete genome sequence. *Nature* 393, 537–544.
- (10) Fleischmann, R. D., Alland, D., Eisen, J. A., Carpenter, L., White, O., Peterson, J., DeBoy, R., Dodson, R., Gwinn, M., Haft, D., Hickey, E., Kolonay, J. F., Nelson, W. C., Umayam, L. A., Ermolaeva, M., Salzberg, S. L., Delcher, A., Utterback, T., Weidman, J., Khouri, H., Gill, J., Mikula, A., Bishai, W., Jacobs, W. R., Jr., Venter, J. C., and Fraser, C. M. (2002) Whole-genome comparison of *Mycobacterium tuberculosis* clinical and laboratory strains. *J. Bacteriol.* 184, 5479–5490.
- (11) Zaunbrecher, M. A., Sikes, R. D., Jr., Metchock, B., Shinnick, T. M., and Posey, J. E. (2009) Overexpression of the chromosomally encoded aminoglycoside acetyltransferase eis confers kanamycin resistance in *Mycobacterium tuberculosis*. *Proc. Natl. Acad. Sci. U.S.A.* 106, 20004–20009.
- (12) Wei, J., Dahl, J. L., Moulder, J. W., Roberts, E. A., O'Gaora, P., Young, D. B., and Friedman, R. L. (2000) Identification of a *Mycobacterium tuberculosis* gene that enhances mycobacterial survival in macrophages. *J. Bacteriol.* 182, 377–384.
- (13) Chen, W., Biswas, T., Porter, V. R., Tsodikov, O. V., and Garneau-Tsodikova, S. (2011) Unusual regioversatility of acetyltransferase Eis, a cause of drug resistance in XDR-TB. *Proc. Natl. Acad. Sci. U.S.A.* 108, 9804–9808.

- (14) Green, K. D., Chen, W., and Garneau-Tsodikova, S. (2012) Identification and characterization of inhibitors of the aminoglycoside resistance acetyltransferase Eis from *Mycobacterium tuberculosis*. *ChemMedChem* 7, 73–77.
- (15) Green, K. D., Chen, W., Houghton, J. L., Fridman, M., and Garneau-Tsodikova, S. (2010) Exploring the substrate promiscuity of drug-modifying enzymes for the chemoenzymatic generation of N-acetylated aminoglycosides. *ChemBioChem* 11, 119–126.
- (16) O'Connor, S., Lam, L. K. T., Jones, N. D., and Chaney, M. O. (1976) Apramycin, a unique aminocyclitol antibiotic. *J. Org. Chem.* 41, 2087–2092.
- (17) Szilágyi, L., and Pusztahelyi, Z. S. (1992) Apramycin: Complete ¹H and ¹³C NMR assignments and study of the solution conformation by ROESY measurements. *Magn. Reson. Chem.* 30, 107–117.
- (18) Williams, J. W., and Northrop, D. B. (1978) Kinetic mechanisms of gentamicin acetyltransferase I. Antibiotic-dependent shift from rapid to nonrapid equilibrium random mechanisms. *J. Biol. Chem.* 253, 5902–5907.
- (19) Magnet, S., Lambert, T., Courvalin, P., and Blanchard, J. S. (2001) Kinetic and mutagenic characterization of the chromosomally encoded *Salmonella enterica* AAC(6')-Iy aminoglycoside N-acetyltransferase. *Biochemistry* 40, 3700–3709.
- (20) Magalhaes, M. L., and Blanchard, J. S. (2005) The kinetic mechanism of AAC3-IV aminoglycoside acetyltransferase from *Escherichia coli*. *Biochemistry* 44, 16275–16283.
- (21) Martel, A., Masson, M., Moreau, N., and Le Goffic, F. (1983) Kinetic studies of aminoglycoside acetyltransferase and phosphotransferase from *Staphylococcus aureus* RPAL. Relationship between the two activities. *Eur. J. Biochem.* 133, 515–521.
- (22) Hegde, S. S., Javid-Majd, F., and Blanchard, J. S. (2001) Overexpression and mechanistic analysis of chromosomally encoded aminoglycoside 2'-N-acetyltransferase (AAC(2')-Ic) from *Mycobacterium tuberculosis*. *J. Biol. Chem.* 276, 45876–45881.
- (23) Kim, C., Villegas-Estrada, A., Heseck, D., and Mobashery, S. (2007) Mechanistic characterization of the bifunctional aminoglycoside-modifying enzyme AAC(3)-Ib/AAC(6')-Ib' from *Pseudomonas aeruginosa*. *Biochemistry* 46, 5270–5282.
- (24) Kim, C., Heseck, D., Zajicek, J., Vakulenko, S. B., and Mobashery, S. (2006) Characterization of the bifunctional aminoglycoside-modifying enzyme ANT(3'')-Ii/AAC(6')-Iid from *Serratia marcescens*. *Biochemistry* 45, 8368–8377.
- (25) Draker, K. A., Northrop, D. B., and Wright, G. D. (2003) Kinetic mechanism of the GCN5-related chromosomal aminoglycoside acetyltransferase AAC(6')-Ii from *Enterococcus faecium*: Evidence of dimer subunit cooperativity. *Biochemistry* 42, 6565–6574.
- (26) Han, Q., Zhao, Q., Fish, S., Simonsen, K. B., Vourloumis, D., Froelich, J. M., Wall, D., and Hermann, T. (2005) Molecular recognition by glycoside pseudo base pairs and triples in an apramycin-RNA complex. *Angew. Chem., Int. Ed.* 44, 2694–2700.
- (27) Hermann, T., Tereshko, V., Skripkin, E., and Patel, D. J. (2007) Apramycin recognition by the human ribosomal decoding site. *Blood Cells, Mol. Dis.* 38, 193–198.
- (28) Kondo, J., Francois, B., Urzhumtsev, A., and Westhof, E. (2006) Crystal structure of the *Homo sapiens* cytoplasmic ribosomal decoding site complexed with apramycin. *Angew. Chem., Int. Ed.* 45, 3310–3314.